ChemComm

COMMUNICATION

View Article Online
View Journal | View Issue

Cite this: *Chem. Commun.*, 2015, 51, 8935

Received 12th March 2015,
Accepted 23rd April 2015

DOI: 10.1039/c5cc02129d

www.rsc.org/chemcomm

Modular design of SPIRO-OMeTAD analogues as hole transport materials in solar cells†

Alexander T. Murray,‡ Jarvist M. Frost,‡ Christopher H. Hendon,‡ Christopher D. Molloy, David R. Carbery and Aron Walsh*

We predict the ionisation potentials of the hole-conducting material SPIRO-OMeTAD and twelve methoxy isomers and polymethoxy derivatives. Based on electronic and economic factors, we identify the optimal compounds for application as p-type hole-selective contacts in hybrid halide perovskite solar cells.

Considerable scientific effort has been focused on the challenge of converting sunlight to electricity. Recently, solution-processed hybrid perovskite based solar cells have reached power conversion efficiencies of 20.1%, values competitive with the mature silicon technologies.[1–10] A critical component of any solar cell (or optoelectronic device) is the electrical contact, which needs to efficiently and selectively extract electrons or holes from the active layer. In order to maximise the photovoltage and photocurrent, the energy levels of the contacts should be well-matched to the active layer of the device.[11] As new hybrid perovskites and alternative absorber layers are being developed for solar cells, beyond the widely employed $CH_3NH_3PbI_3$, the ability to modulate the energy levels of the selective contacts to match those of the absorber[12] will be essential in order to maximise power conversion efficiency.

Most high-efficiency hybrid perovskite solar cells use the hole conductor $N^2,N^2,N^{2\prime},N^{2\prime},N^7,N^7,N^{7\prime},N^{7\prime}$-octakis(4-methoxyphenyl)-9,9′-spirobi[9*H*-fluorene]-2,2′,7,7′-tetramine (SPIRO-OMeTAD, Fig. 1a).[14,15] SPIRO-OMeTAD is widely used in solution processed solar cells with an ionisation potential well matched to a number of active (light absorbing) layers. The material forms an amorphous glass, rather than a partially crystalline phase, enabling smooth films to be formed.[16]

Electronic energy level alignment is important for solar cells, but is commonly used in post-rationalisation of successful architectures rather than as a design principle *a priori*. One compelling example was recently presented by Seok and co-workers, where the energy levels of SPIRO-OMeTAD were tuned by altering the connectivity of the methoxy ethers on the amino phenyl motifs.[17] Similarly, other groups are interested in the computational design of contacts for more mature photovoltaic technologies.

From the study of Seok, it was concluded that the geminal *ortho*-methoxyphenyl, *para*-methoxyphenyl arrangement produced a cell with +2% boost in conversion efficiency relative the typical SPIRO-OMeTAD (geminal *para*-methoxyphenyl, *para*-methoxyphenyl).

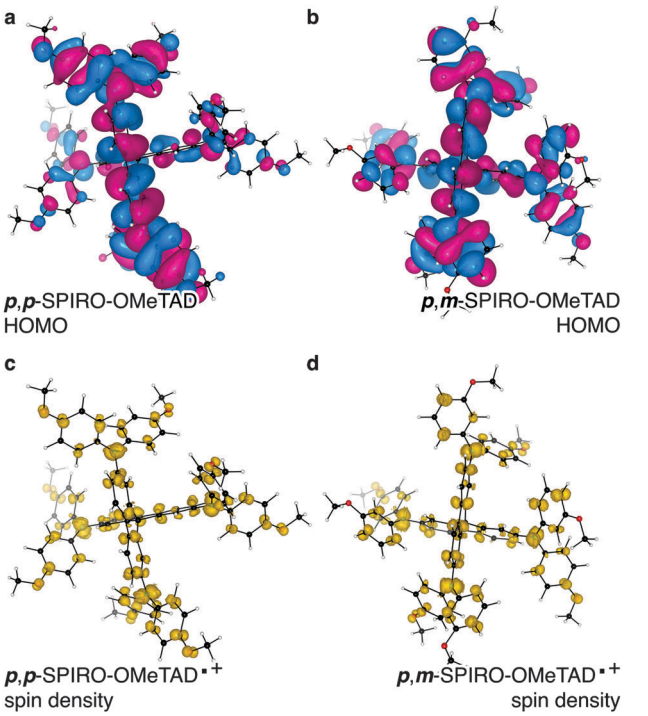

Fig. 1 Calculated *p,p*-SPIRO-OMeTAD highest-occupied molecular orbital (HOMO) (a) and the associated one electron oxidised spin density (c) and *p,m*-SPIRO-OMeTAD HOMO (b) and the associated one electron oxidised spin density (d). The plots were made with a HOMO isovalue = 0.03 e Å^{-3} and spin-density isovalue = 0.01 e Å^{-3} in the code VESTA.[13]

Department of Chemistry, University of Bath, Claverton Down, Bath, BA2 7AY, UK. E-mail: a.walsh@bath.ac.uk

† Electronic supplementary information (ESI) available: Full cost analysis and computational methods. See DOI: 10.1039/c5cc02129d

‡ These authors contributed equally to this work and hence share first authorship.

They also found that the geminal *meta*-methoxyphenyl, *para*-methoxyphenyl isomer was detrimental to hole conduction. This increase in efficiency was correlated with an increase in oxidation potential as estimated from cyclic voltammetry, which has limited accuracy. Careful measurements using techniques such as differential pulse voltammetry (which allows for low concentration voltammetry measurements, avoiding aggregation) would allow more accurate and informative measurements with the broadly the same experimental setup.[18] Variation in device-to-device performance, and issues such as implicit doping[19] from various syntheses of hybrid or organic electronic materials, means that it requires extremely large study to provide the definitive answer of which material is optimal.

In solar cells, SPIRO-OMeTAD can be used in the neutral, one and two electron oxidised forms. Chemical doping with lithium salts is typically performed to increase conductivity.[20] Fig. 1 shows the Kohn–Sham highest occupied molecular orbital (HOMO) of the neutral, and the singly-occupied molecular orbital (SOMO) of the cationic radical state of the most common SPIRO-OMeTAD isomer (*p*,*p*-SPIRO-OMeTAD), as well as the *p*, *m* isomer previously found to be detrimental. These frontier orbitals provide a qualitative interpretation of the chemical bonding. Both the HOMO and SOMO show similar electronic structure: the electron density is centred on the extended π network, primarily on the carbons.

The oxidised doublet state can be viewed as the removal of an electron from this π system; the associated spin density is centred again on the carbon system, but there is significant spin stabilisation from the heteroatoms (*i.e.* N). Additionally, the amino phenyl carbons, as defined by the position of the methoxy ether motifs, do not appear to affect the contribution to the delocalised radical. This effect is notable as the amino phenyl motifs are not part of the extended π system due to the violation of Hückel planarity.[21]

Due to the lack of π planarity, we would not expect organic modifications to affect the ionisation potential to the extent we observe for typical planar conjugated systems.[22] This suggests that isomer modifications should allow for energy level modulation, within a narrow range, through repositioning of the methoxy ether motifs.[23,24]

To investigate the possible synthetic scope in modifying the side chains, we have predicted the energy level alignment of *p*,*p*-SPIRO-OMeTAD and 12 structurally related isomers (Fig. 3). These calculations are by hybrid density functional theory (DFT) with atom-centered numerical basis functions (see ESI† for full details). We report both the Kohn–Sham energy gap (from B3LYP), and more reliable ionisation potentials were calculated with the delta self-consistent field (ΔSCF) method. All calculations were of a single molecule in the gas phase, as we were looking for relative variations in the ionisation potential, rather than an absolute value for the solid state, which may be influenced by molecular packing. We do not consider these values to be definitive. More accurate model chemistries might achieve more precise gas phase values, but the variation caused by solid state packing in the real system would have more of an effect on device performance and the overall accuracy of such predictions.

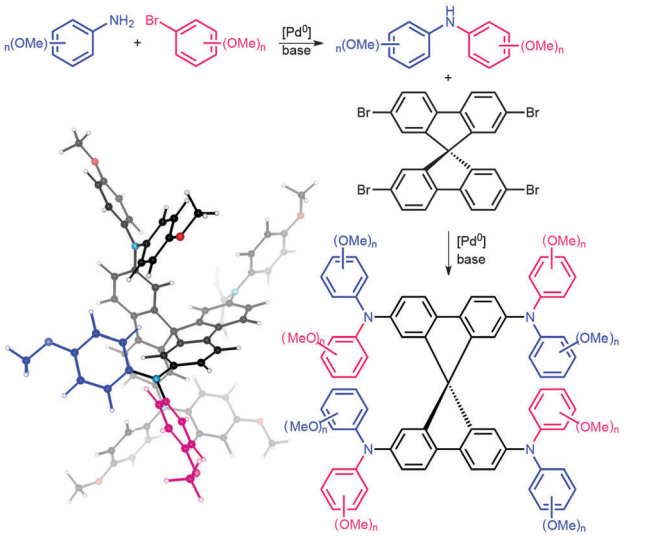

Fig. 2 Sequential synthesis of SPIRO-OMeTAD derivatives and B3LYP optimised geometry of *p*,*p*-SPIRO-OMeTAD with r_1 and r_2 highlighted in blue and pink.

As detailed in Fig. 2, we defined the two aminoaryl rings as r_1 and r_2, and used *o*, *m*, and *p* to refer to regiochemistry relative to the amine (or bromide). These correspond to the 2-, 3- and 4-positions, respectively. The predicted electronic modulation is modest, but important in the context of efficient hole extraction. Two important conclusions can be made: (i) *meta*-methoxy substitutions result in generally increased ionisation potentials, as the contribution of the oxygen donation is reduced with reduced structural symmetry (lowering the energy of the π system); (ii) *para*- and *ortho*-substituted derivatives result in decreased ionisation potentials due to the increased energy of the π system. In the cases of poly-OMe substitutions, the decreased ionisation potential is also realised by the repulsive interaction between neighbouring rings.

The Kohn–Sham energy gap (E_g, written in colour in Fig. 3) is relatively constant for all isomers. Here, the HOMO eigenvalue deviates from our ΔSCF ionisation potential, suggesting that Koopman's approximation is insufficient for predicting even qualitative trends. However, our ΔSCF calculations are in close agreement with the experimentally determined ionisation potential for the *p*,*p*-analogue,[25] and with the *p*,*m*-analogue,[17] though we contradict experiment and predict that the *p*,*o*-analogue[17] should see an enhancement.

An especially interesting molecule is the case in which $r_1 = r_2 = o,o$. This derivative has a notably smaller ionisation potential than other analogues, which is likely due to both the electron donating contribution of the *ortho*-positions and 'through-space' conjugation to the amine motif.[26]

Tuning the energy levels in a contact material is only a partial fulfilment of the requirements – we also need to transport the holes efficiently, and so avoid surface recombination. Calculating charge carrier transport for a novel organic material is

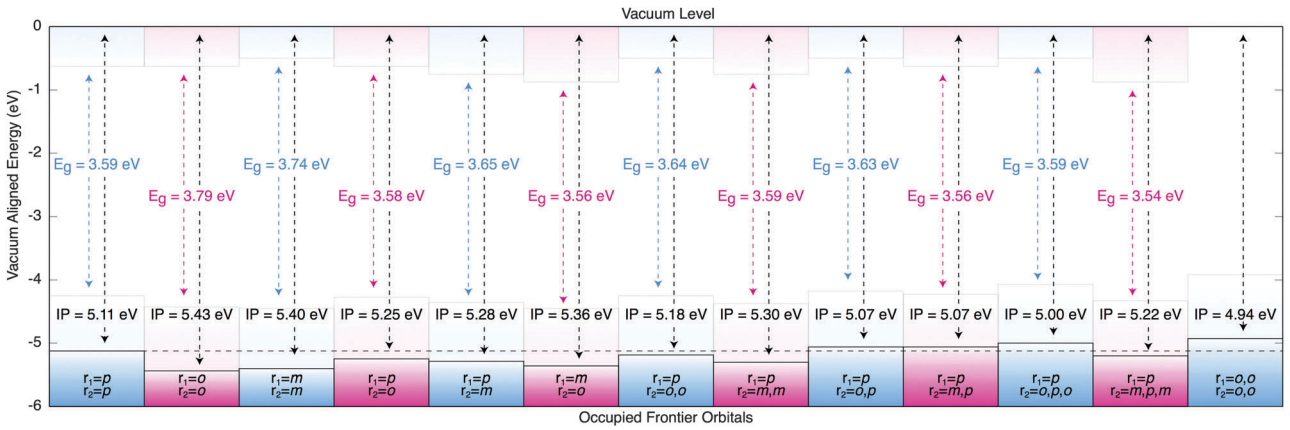

Fig. 3 The calculated single-particle Kohn–Sham energy gaps (E_g) and ΔSCF ionisational potentials (IP) for a range of SPIRO-OMeTAD derivatives (as defined in Fig. 2). The black dashed horizontal line refers to the IP of *p*,*p*-SPIRO-OMeTAD.

extremely difficult, as a full model of packing and an understanding of the dielectric environment is required before microscopic charge transfer integrals can be calculated and a macroscopic mobility predicted.[27] One expects that adding bulky side chains would decrease the molecular packing density and coordination number, and so reduce the electronic overlap and thus microscopic mobility.

A barrier to the large-scale production of novel solar cells is the cost of SPIRO-OMeTAD. This can be partially attributed to the recent fluctuations in supply and demand, but is also due to the cost of the starting materials. A typical synthesis of SPIRO-OMeTAD begins with the Pd-catalysed coupling of anisidine (*para*-methoxyaniline) and *para*-methoxybromobenzene to form a secondary aniline. Four equivalents of the aniline are then resubjected to similar coupling conditions with the brominated spiro core; 2,2′,7,7′-tetrabromo-9,9′-spirobi[9*H*-fluorene], Fig. 2, forming *p*,*p*-SPIRO-OMeTAD.[17] In principle, any commercially available aniline and aryl bromide could be used to construct a diverse library of electronically dissimilar SPIRO-OMeTAD derivatives. Assuming isomer transferable reaction conditions (*i.e.* the use of the same catalysts, purification methods and yields) we have included a rudimentary cost break down associated with the reagents required for our library (see ESI† for a full cost analysis).

Beyond the cases considered here, greater electronic variability should be achievable through substitution about the fluorene core (direct conjugation modulation). However, given the current lack of commercial availability of alternate core materials, this could be a more synthetically challenging endeavour. Recent advances in aryl C–H activation chemistry could find a useful application in the functionalisation of these molecules.[28–31]

In conclusion, we have calculated the ionisation potentials of a variety of analogues of the hole conducting material SPIRO-OMeTAD, varying the HOMO energy through alterations to the positioning of methoxy groups on the pendant aryl rings of the molecule. Our method is computationally efficient, has been shown to offer good agreement with experimental measures from solution voltammetry. We predict that these synthetic variants offer flexibility in work function matching for solar cell design and optimisation, and that the majority of analogues could be candidates for large-scale development and application.

We thank K. Tobias Butler for lyrical insights. We acknowledge membership of the U.K.'s HPC Materials Chemistry Consortium, which is funded by EPSRC Grant EP/L000202. Additional support has been received from EPSRC Grants EP/K016288/1 and EP/J017361/1, the Royal Society, and the ERC (Grant no. 277757).

References

1 J. Burschka, N. Pellet, S.-J. Moon, R. Humphry-Baker, P. Gao, M. K. Nazeeruddin and M. Grätzel, *Nature*, 2013, **499**, 316.
2 O. Malinkiewicz, A. Yella, Y. H. Lee, G. M. Espallargas, M. Grätzel, M. K. Nazeeruddin and H. J. Bolink, *Nat. Photonics*, 2014, **8**, 128.
3 A. Kojima, K. Teshima, Y. Shirai and T. Miyasaka, *J. Am. Chem. Soc.*, 2009, **131**, 6050.
4 N. J. Jeon, J. Lee, J. H. Noh, M. K. Nazeeruddin, M. Grätzel and S. I. Seok, *J. Am. Chem. Soc.*, 2013, **135**, 19087.
5 J. M. Frost, K. T. Butler, F. Brivio, C. H. Hendon, M. van Schilfgaarde and A. Walsh, *Nano Lett.*, 2014, **14**, 2584.
6 C. H. Hendon, R. X. Yang, L. A. Burton and A. Walsh, *J. Mater. Chem. A*, 2015, **3**, 9067.
7 M. J. Carnie, C. Charbonneau, M. L. Davies, J. Troughton, T. M. Watson, K. Wojciechowski, H. Snaith and D. A. Worsley, *Chem. Commun.*, 2013, **49**, 7893.
8 D. S. Bhachu, D. O. Scanlon, E. J. Saban, H. Bronstein, I. P. Parkin, C. J. Carmalt and R. Palgrave, *J. Mater. Chem. A*, 2015, **3**, 9071.
9 B.-W. Park, E. M. J. Johansson, B. Philippe, T. Gustafsson, K. Sveinbjörnsson, A. Hagfeldt and G. Boschloo, *Chem. Mater.*, 2014, **26**, 4466.
10 K. T. Butler, J. M. Frost and A. Walsh, *Energy Environ. Sci.*, 2015, **8**, 838–848.
11 K. T. Butler, P. E. Vullum, A. M. Muggerud, E. Cabrera and J. H. Harding, *Phys. Rev. B: Condens. Matter Mater. Phys.*, 2011, **83**, 235307.
12 K. T. Butler and J. H. Harding, *Phys. Rev. B: Condens. Matter Mater. Phys.*, 2011, **86**, 245319.
13 K. Momma and F. Izumi, *J. Appl. Crystallogr.*, 2008, **41**, 653–658.
14 U. Bach, P. Comte, J. E. Moser, F. Weissörtel, J. Salbeck, H. Spreitzer and M. Grätzel, *Nature*, 1998, **395**, 583.
15 M. M. Lee, J. Teuscher, T. Miyasaka, T. N. Murakami and H. J. Snaith, *Science*, 2012, **338**, 643.
16 F. Fabregat-Santiago, J. Bisquert, L. Cevey, P. Chen, M. Wang, S. M. Zakeeruddin and M. Grätzel, *J. Am. Chem. Soc.*, 2009, **131**, 558.
17 N. J. Jeon, H. G. Lee, Y. C. Kim, J. Seo, J. H. Noh, J. Lee and S. I. Seok, *J. Am. Chem. Soc.*, 2014, **136**, 7837.

18 J. M. Frost, M. A. Faist and J. Nelson, *Adv. Mater.*, 2010, **22**, 4881.
19 T. Kirchartz and J. Nelson, *Phys. Rev. B: Condens. Matter Mater. Phys.*, 2012, **86**, 165201.
20 W. H. Nguyen, C. D. Bailie, E. L. Unger and M. D. McGehee, *J. Am. Chem. Soc.*, 2014, **136**, 10996.
21 E. Hückel, *Z. Phys.*, 1931, **70**, 204.
22 C. H. Hendon, D. Tiana, M. Fontecave, C. Sanchez, L. D'arras, C. Sassoye, L. Rozes, C. Mellot-Draznieks and A. Walsh, *J. Am. Chem. Soc.*, 2013, **135**, 10942.
23 A. T. Murray, P. Matton, N. W. G. Fairhurst, M. P. John and D. R. Carbery, *Org. Lett.*, 2012, **14**, 3656.
24 C. H. Hendon, D. R. Carbery and A. Walsh, *Chem. Sci.*, 2014, **5**, 1390.
25 H.-S. Kim, C.-R. Lee, J.-H. Im, K.-B. Lee, T. Moehl, A. Marchioro, S.-J. Moon, R. Humphry-Baker, J.-H. Yum, J. E. Moser, M. Grätzel and N.-G. Park, *Sci. Rep.*, 2012, **2**, 1.
26 C. R. Martinez and B. L. Iverson, *Chem. Sci.*, 2012, **3**, 2191.
27 J. Nelson, J. J. Kwiatkowski, J. Kirkpatrick and J. M. Frost, *Acc. Chem. Res.*, 2009, **42**, 1768.
28 F. W. Patureau, C. Nimphius and F. Glorius, *Org. Lett.*, 2011, **13**, 6346.
29 J. Wencel-Delord, C. Nimphius, F. W. Patureau and F. Glorius, *Chem. – Asian J.*, 2012, **7**, 1208.
30 H. Wang, C. Grohmann, C. Nimphius and F. Glorius, *J. Am. Chem. Soc.*, 2012, **134**, 19592.
31 C. Arroniz, J. G. Denis, A. Ironmonger, G. Rassias and I. Larrosa, *Chem. Sci.*, 2014, **5**, 3509.